Hepat Mon. 2026 December; 26(1): e166157 https://doi.org/10.5812/hepatmon-166157

Published Online: 2026 February 10 **Research Article**

USP7 Enhances Epithelial Mesenchymal Transition and Cancer Stem Cell-Like Properties in Hepatocellular Carcinoma by the AKT/β-Catenin Pathway: A Randomized Trial

Mingchao Hu [1], Yuhong Zhu [1], Lili Wang [1], Huilan Ye [1], Rongcan Xu [1], Jinlong Zhai [1], Linlin Yang [1], Xingtao Jin [1,*]

[1] Sheyang People's Hospital, Yancheng, China

[*] ***Corresponding Author:*** Sheyang People's Hospital, Yancheng, China. Email: jxt1536576_66@hotmail.com

Received: 7 September, 2025; **Revised:** 29 November, 2025; **Accepted:** 24 December, 2025

Abstract

Background: The malignant progression of hepatocellular carcinoma (HCC) is closely linked to the epithelial-mesenchymal transition (EMT) process and cancer stem cells (CSCs) characteristics. Ubiquitin-specific protease 7 (USP7) is found to be elevated in various tumors, but its molecular mechanism for regulating EMT and CSCs in HCC has not been fully elucidated.

Objectives: To investigate whether USP7 affects the EMT process and CSCs characteristics in HCC cells via regulation of the AKT/β-catenin pathway.

Methods: Twenty-four Balb/c nude mice were randomly assigned to the OE-USP7, OE-NC, sh-USP7, or sh-NC groups using a random number table method (n=6 mice in each group), and 200 µL of Huh-7 cell suspension transfected with OE-USP7, OE-NC, sh-USP7, or sh-NC was injected into mice to establish the HCC model, respectively. The OE-NC group and sh-NC group served as controls for the OE-USP7 and sh-USP7 groups, respectively. Blinding procedures were implemented throughout the experiment: the researchers responsible for nude mouse feeding and tumor growth monitoring (measuring tumor volume weekly) were blinded to the grouping information. On the 28th day, mice were euthanized, and the proliferation marker Ki-67 in tumors was assessed by immunohistochemistry. Immunofluorescence and Western blot detected USP7 expression in THLE-2, HCCLM3, and Huh-7 cells. Cell proliferation, migration, invasion ability, and stemness were examined through cell counting kit-8 (CCK-8), Transwell, and sphere formation assays. Flow cytometry was utilized to analyze CSCs markers. Western blot detected AKT/β-catenin pathway proteins, EMT markers, and stemness factors levels.

Results: Compared with normal hepatocytes, USP7 level in HCC cells was remarkably higher ($P < 0.05$). Overexpression of USP7 increased cell viability, globulation, and CSCs characteristics, and facilitated migratory invasion and EMT process in HCC cells, while knockdown of USP7 inhibited the above phenotypes ($P < 0.05$). Overexpression of USP7 activated the AKT/β-catenin pathway, but knockdown of USP7 blocked this pathway. PI3K inhibitors attenuated the enhancing impact of overexpression of USP7 on the EMT process and CSCs characterization in HCC cells ($P < 0.05$). Additionally, knockdown of USP7 reduced both the size and weight of tumor tissues in vivo, decreased the Ki67 positivity rate, and inhibited the EMT process and CSCs characteristics.

Conclusions: USP7 enhances the properties of CSCs and promotes cell proliferation and EMT process in HCC cells through regulation of the AKT/β-catenin pathway.

Keywords: Hepatocellular Carcinoma, USP7, Epithelial-Mesenchymal Transition, Cancer Stem Cells, AKT/β-catenin Pathway

1. Background

Liver cancer is the third most common cause of cancer-related mortality globally and the sixth most prevalent malignant tumor (1, 2). Hepatocellular carcinoma (HCC) represents the predominant form of liver malignancy, constituting approximately 90% of primary liver cancer cases (3). Hepatocellular carcinoma

How to Cite: Hu M, Zhu Y, Wang L, Ye H, Xu R, et al. USP7 Enhances Epithelial Mesenchymal Transition and Cancer Stem Cell-Like Properties in Hepatocellular Carcinoma by the AKT/β-Catenin Pathway: A Randomized Trial. Hepat Mon. 2026;26(1):e166157. doi: https://doi.org/10.5812/hepatmon-166157

exhibits significant heterogeneity, with nonspecific early symptoms, insidious onset, and rapid progression. Most patients are diagnosed at an advanced stage, and tumor recurrence and metastasis are primary causes of poor prognosis, resulting in a five-year survival rate below 20% (4, 5). Although current tumor treatments have made great progress, HCC is highly invasive, prone to metastasis and recurrence, and its five-year survival rate is still very low, only 10% (6-8). With their capacity for differentiation and self-renewal, cancer stem cells (CSCs) also exhibit strong invasive and migratory features (9). The CSCs-like properties of HCC and epithelial-mesenchymal transition (EMT) are not only major drivers of tumor heterogeneity, but also of drug resistance and recurrence (10, 11). Therefore, exploring the regulatory mechanisms of CSCs-like properties and EMT against HCC and identifying new molecular targets are crucial for the clinical diagnosis and drug development of HCC.

Ubiquitination is an important protein post-translational modification process that is vital for regulating tumor metastasis as well as CSCs-like properties (12-14). Ubiquitin-specific protease 7 (USP7) is a member of the USP deubiquitinating enzyme family, which removes ubiquitin from specific protein substrates and recovers proteins from proteasomal degradation (15). Ubiquitin-specific protease 7 is involved in key physiological processes, such as cell cycle regulation, DNA damage repair, and immune response (16, 17). Research has now reported that inhibitors targeting USP7 have potential for tumor treatment (18, 19). Notably, USP7 shows a marked increase in expression within HCC, especially among patients suffering from advanced HCC, and its high-expressing patients have lower 5-year survival rates than low-expressing ones (20). In a previous study, we found that USP7 interacts with basic transcription factor 3 (BTF3) and stabilizes BTF3, thereby enhancing the CSCs-like characteristics of HCC cells (21). However, at present, studies on USP7 in HCC are still insufficiently in-depth, and its mechanism of action has not been completely understood.

Various investigations have indicated that the AKT/β-catenin pathway is abnormally activated in several malignant tumors, including HCC, gastric cancer, and oral cavity cancer (22-24). Yang et al. reported that stimulation of the AKT/β-catenin pathway increased chemoresistance and enhanced CSCs-like properties in HCC cells, whereas intervention with pathway inhibitors decreased the expression of CSCs marker proteins (CD24 and CD133) (25). In addition, promoting the stimulation of the EGFR/AKT/β-catenin pathway also promotes the EMT process in HCC cells (26). Previous studies have demonstrated that targeting specific molecular pathways, such as the apoptosis pathway (27), constitutes a validated therapeutic strategy. Findings from these investigations highlight the significant involvement of the AKT/β-catenin pathway in the stem cell-like traits and the EMT process of HCC cells. Therefore, we investigated the role of USP7 in influencing the EMT process and CSCs-like properties of HCC cells by modulating the AKT/β-catenin signaling pathway, which subsequently facilitates HCC malignant progression.

2. Objectives

This work aims to elucidate the specific mechanism of action of USP7 in regulating the malignant progression of HCC, and to provide some experimental basis for creating combined treatment approaches that target USP7 and its downstream pathways.

3. Methods

3.1. Cell Culture

Human normal liver epithelial cells THLE-2 (CL-0833), HCC cell lines HCCLM3 (CL-0278) and Huh-7 (CL-0120) were from Pricella Biotechnology (Wuhan, Hubei, China). THLE-2 cells were maintained in THLE-2-specific medium (CM-0833, Pricella Biotechnology). Hepatocellular carcinoma cells were grown in complete medium containing 10% fetal bovine serum (FBS, A5256701, Gibco, Grand Island, NY, USA), 1% penicillin/streptomycin (15140122, Gibco), and 89% DMEM (12491015, Gibco). The incubation temperature was 37°C in an environment containing 5% CO_2. Fluid was changed 2-3 times per week and the passaging ratio was 1:3.

Ubiquitin-specific protease 7 overexpression plasmid (OE-USP7), USP7 short hairpin RNA (sh-USP7), and their controls (OE-NC, sh-NC) were synthesized by Sangon Biotech Co. Ltd. (Shanghai, China). Hepatocellular carcinoma cells were digested by 0.25% trypsin (T2605, Sigma-Aldrich, St. Louis, MO, USA), then inoculated in 24-well plates (2×10^4/well). On the second day, the transfection system was prepared according to the guidelines provided for Lipofectamine 3000 (L3000001, Invitrogen, Carlsbad, CA, USA). Fifty microliters of the configured transfection system was mixed well with HCC cells in a 24-well plate, and after 48 h of reaction, the cells were lysed with RIPA lysis buffer (15596026, Invitrogen). Proteins were fully extracted, and the effectiveness of the transfection was assessed by

measuring USP7 protein level in the cells, and subsequent cellular experiments were performed.

For signaling pathway exploration, HCC cells were exposed to the PI3K activator 740Y-P (30 μM, HY-P0175, MedChemExpress, Monmouth Junction, NJ, USA) or the PI3K inhibitor LY294002 (25 μM, HY-10108, MedChemExpress) for 1 h, then transfected with OE-USP7, recorded as OE-USP7+LY294002 group or OE-USP7+740Y-P group (28, 29).

3.2. Immunofluorescence

Hepatocellular carcinoma cells were seeded into 6-well plates (with built-in sterile coverslips), and when the cells grew to a density of 50%-60%, the cell crawls were treated with 4% paraformaldehyde (441244, Sigma-Aldrich) for 20 min. After that, 0.3% Triton X-100 (T824275, Macklin Inc., Shanghai, China) was added to the surface of cell crawls and incubated for 10 min to increase the permeability of the cell membrane. It was blocked with 5% bovine serum albumin (BSA, A801320, Macklin Inc.) for 30 min. Subsequently, cells were exposed to primary antibodies USP7 (PA5-34911, 1:200, Invitrogen, Carlsbad, CA, USA), E-cadherin (PA5-32178, 1:200, Invitrogen), and Vimentin (PA5-27231, 1:500, Invitrogen) at 4°C overnight. The following day, cells were exposed to secondary antibody goat anti-rabbit IgG (65-6111, 1:2000, Invitrogen) for 60 min in the dark at 37°C. After that, cells were incubated with DAPI solution (C1005, Beyotime, Shanghai, China) for 10 min, and then observed through a BX53 (LED) fluorescence microscope (Olympus, Tokyo, Japan).

3.3. Cell Counting Kit-8 Assay

Huh-7 and HCCLM3 cells transfected with OE-USP7, sh-USP7, or their control vectors in good growth status were taken and seeded into 96-well plates (1.0×10^4 cells/well, 100 μL). Once the cells had completely adhered, 10% cell counting kit-8 (CCK-8) reagent (96992, Sigma-Aldrich) was added at 24, 48, 72, and 96 h. After mixing well, the cells were allowed to incubate for 2 h at a temperature of 37°C, and OD450 values were measured through a microplate reader (1410101, Thermo Fisher Scientific, Waltham, MA, USA). In addition, cell morphology was observed with a CX33 light microscope (Olympus) to assess cell viability.

3.4. Transwell Assay

Matrigel (HY-K6002, MedChemExpress) was melted at ambient temperature and mixed with culture medium. One hundred microliters of diluted matrix gel was aspirated and uniformly covered on the basement membrane of the Transwell (8 μm, Corning, Tewksbury, MA, USA). After the matrix gel solidified naturally for 30 min at 37°C, the chambers were transferred to 24-well cell culture plates. Subsequently, complete medium (500 μL) was dispensed into the lower chamber, followed by the addition of 100 μL of HCCLM3 and Huh-7 cell suspensions to the upper chamber, then incubated for 24 h at 37°C. After incubation, Transwell chambers were carefully retrieved. Subsequently, the chambers were rinsed twice with PBS, and gently wiped with a sterile cotton swab to remove non-invaded cells adhering to the upper surface of the matrix gel. Subsequently, the chambers were immersed in 4% paraformaldehyde for fixation for 15 min and rinsed under running water for 2 min. The invaded cells were exposed to 0.1% crystal violet (C805211, Macklin Inc.) for 15 min, then rinsed slowly with running water for 2 min and dried naturally. A light microscope was used to capture images of five randomly chosen fields of view from each chamber, and the invaded cell count was recorded using Image J 1.54h software (Wavne Resband, National Institute of Mental Health, USA).

Transwell migration assay did not require the addition of Matrigel matrix gel to the chambers, and all other experimental procedures and analysis were aligned with those of the invasion assay.

3.5. Flow Cytometry

HCCLM3 and Huh-7 cells were collected by centrifugation in 5 mL centrifuge tubes. Cells were resuspended by adding PBS buffer containing 1% FBS to make a single-cell suspension (approximately 1.0×10^6/mL). FITC-labeled CD44 antibody (11-0441-82, Invitrogen) and PE-labeled CD133 antibody (12-1331-82, Invitrogen) were added and mixed well, then incubated at 4°C for 30 min under light protection (30). The samples were then transferred to a BD FACSCaliburTM flow cytometer (BD Biosciences, San Jose, CA, USA) for fluorescence cell sorting analysis. Subsequently, the proportion of positive cells was quantified using FlowJo software (version 10.8, BD Biosciences).

3.6. Cancer Stem Cells Sphere Formation Assay

Tumor cell spheroid formation assay is the gold standard for measuring tumor cell stemness. DMEM medium was supplemented with insulin (4 μg/mL, P3376, Beyotime), 1 × B-27 (17504044, Gibco), human recombinant epidermal growth factor protein (EGF, 20 ng/mL, HY-P72982, MedChemExpress), and human recombinant fibroblast growth factor protein (FGF, 20 ng/mL, GF003, Sigma-Aldrich), and formulated into cell-

forming medium (31). After Huh-7 cells were digested and resuspended, they were rinsed twice with PBS and inoculated in 24-well ultra-low adhesion culture plates (1×10^4/well). After 7-10 days of culture, most spheroplasts were observed to grow to more than 100 μm for counting, and the spheroplast formation efficiency was calculated (32).

3.7. Subcutaneous Tumor Formation in Nude Mice

Male Balb/c nude mice (15 - 19 g, 6 weeks old) were from Vitalriver (Beijing, China). The animals were maintained at 22°C, and were free to eat and drink, and the experiments were conducted after one week of acclimatization. Animals were split into 4 groups (n = 6) using a random number table method, and 200 μL of Huh-7 cell suspension transfected with OE-USP7, OE-NC, sh-USP7, or sh-NC was injected into the right axilla of nude mice in each group (5.0×10^6 cells/mice), respectively (33). On days 7, 14, 21, and 28 after the Huh-7 cell suspension was injected, the dimensions of subcutaneous tumors were examined using vernier calipers. On the 28th day, all nude mice underwent execution via an intraperitoneal injection of sodium pentobarbital (100 mg/kg). The tumors were entirely excised using tissue shears, then weighed and photographed for record. To minimize bias, a double-blind approach was adopted. All the researchers involved in animal breeding, model construction, behavioral assessment, and pathological section staining were unaware of the grouping situation.

3.8. Immunohistochemistry

Mouse tumor tissues were immersed in 4% paraformaldehyde for 24 h to fix them, followed by a dehydration procedure with graded ethanol, embedding in paraffin, and sectioning into 4 μm-thick slices for subsequent analysis. Subsequently, sections were put into xylene (X821391, Macklin Inc.) for deparaffinization, hydrated in gradient ethanol, and then washed using distilled water. The antigens were microwave repaired by placing sections in citric acid solution (pH = 6, 0.1 mol/L). The tissue sections were incubated in 3% H_2O_2 solution for 30 min, and then covered evenly with 5% BSA and blocked for 30 min. Subsequently, Ki67 primary antibody (PA1-38032, 1:100, Invitrogen) was introduced and allowed to incubate at 37°C for 90 min. Subsequently, sections were incubated with horseradish peroxidase (HRP)-labeled goat anti-rabbit IgG (31460, 1:500, Invitrogen) for 20 min at 25°C. The color development reaction was carried out using DAB (P0203, Beyotime), and the color development was terminated with distilled water when the color development reached the desired effect. Hematoxylin (H9627, Sigma-Aldrich) was restained for 5 min, rinsed in distilled water, and the samples were visualized using a fluorescence microscope after blocking with Neutral Balsam (C0173, Beyotime).

3.9. Western Blot

Tumor tissues were cut with tissue shears, ground thoroughly, and mixed well with RIPA lysis buffer. Hepatocellular carcinoma cells were rinsed two times with PBS, and mixed well with RIPA lysis buffer. After completion of lysis, protein contents in tissues and cells were examined through the bicinchoninic acid (BCA) protein assay kit (P0012, Beyotime). Next, proteins were separated by SDS-PAGE electrophoresis, and the proteins were transferred to PVDF membranes (Invitrogen), then blocked with 5% BSA for 2 h. Subsequently, the membranes underwent an overnight incubation with primary antibodies SOX2 (PA1-094, 1:1000, Invitrogen), USP7 (PA5-34911, 1:2000, Invitrogen), E-cadherin (PA5-32178, 1:500, Invitrogen), Vimentin (ab16700, 1:1000, Abcam, Cambridge, MA, USA), N-cadherin (PA5-19486, 1:100, Invitrogen), Snail (PA5-23482, 1:100, Invitrogen), CD44 (PA5-21419, 1:2000, Invitrogen), C-Myc (PA5-85185, 1:500, Invitrogen), CD133 (PA5-38014, 1:100, Invitrogen), Octamer-binding transcription factor 4 (OCT4, PA1-16943, 1:500, Invitrogen), Nanog (PA1-097, 1:1000, Invitrogen), Krüppel-like factor 4 (KLF4, PA5-27441, 1:5000, Invitrogen), p-AKT (Ser473) (9271S, 1:1000, cell signaling technology, Danvers, MA, USA), glycogen synthase kinase-3β (GSK3β, ab32391, 1:5000, Abcam), AKT (ab81283, 1:5,000, Abcam), β-catenin (MA5-34961, 1:500, Invitrogen) or p-GSK3β (44-604G, 1:1000, Invitrogen) at 4°C. The following day, the membranes were rinsed 3 times, and incubated with the secondary antibody (ab205718, 1:10000, Abcam) for 2 h. Developing solution (HY-K2005, MedChemExpress) was prepared, dropped evenly on the membrane, and then analyzed using the 5200 Multi gel imaging system (Tanon, Shanghai, China). The internal reference GAPDH (ab128915, 1:10000, Abcam) was employed for normalization. Images were processed using Image J 1.54 h software to quantify the gray values of each protein band, from which relative levels were determined by normalizing to the GAPDH signal.

3.10. Statistical analysis

All experimental data were derived from at least three independent replicates and are presented as the mean ± standard deviation. Statistical analyses were performed using SPSS 26.0 software (IBM SPSS Statistics

26). The data were initially analyzed for normality using the Shapiro-Wilk test and for homogeneity of variance via Levene's test. In the two comparisons, parametric data were analyzed using a two-tailed unpaired t-test (with Bonferroni correction applied to P-values for multiple comparisons), whereas nonparametric data were assessed via Mann-Whitney U-test. A one-way analysis of variance (ANOVA) was utilized to evaluate the overall differences between multiple groups, and two-by-two comparisons were performed using Tukey's HSD post hoc test (with built-in multiple comparison correction, controlling the overall type I error rate at $\alpha = 0.05$). $P < 0.05$ represents a statistically significant difference. Plotting was performed using Prism software (Graphpad 9.0).

4. Results

4.1. Ubiquitin-Specific Protease 7 Expression in Hepatocellular Carcinoma and Its Role in Cell Proliferation

Immunofluorescence staining indicated that the fluorescent signal intensity of USP7 was markedly greater in the HCC cells (HCCLM3 and Huh-7) than in THLE-2 cells, suggesting that USP7 expression is upregulated in HCC cells (Figure 1A). Western blot assay revealed a notable increase in the intensity of USP7 protein bands in HCC cell lines compared to THLE-2 cells, with quantitative analysis also indicating elevated USP7 protein expression levels in HCC (Figure 1B). Next, we transfected OE-NC/OE-USP7 as well as sh-NC/sh-USP7 in Huh-7 and HCCLM3 cells, and detected USP7 expression in the transfected cells through immunofluorescence. The intensity of intracellular USP7 fluorescence signal was markedly increased in HCC cells transfected with OE-USP7, while the intensity of USP7 fluorescence signal in cells transfected with sh-USP7 was notably decreased, suggesting that exogenous intervention can effectively regulate USP7 level (Figure 1C). In addition, the USP7 protein level in the OE-USP7 group was notably elevated, whereas the protein level in the sh-USP7 group was decreased, further confirming the validity of the overexpression and knockdown operation for subsequent functional experiments (Figure 1D). Cell counting kit-8 assay revealed that the absorbance values of HCC cells transfected with OE-USP7 showed a continuous increase during 24 - 96 h of culture, suggesting that their proliferative ability was significantly enhanced; on the contrary, the absorbance values in the sh-USP7 group gradually decreased with the extension of the culture time, which indicated that the knockdown of USP7 could effectively inhibit the proliferative activity of HCC cells (Figure 1E-F). Microscopic observation of cell morphology showed that HCC cells in the OE-USP7 group showed more active growth, with clear cell contours and enhanced wall-adhesion ability. In contrast, cells in the sh-USP7 group exhibited reduced cell volume, decreased apposition density, and some cells showed signs of cytoplasmic vacuolization, further corroborating the correlation between USP7 expression level and HCC cell viability (Figure 1G). These findings indicate that USP7 is up-regulated in HCC cells, overexpression of USP7 promotes cell proliferation, whereas knockdown of USP7 inhibits cell proliferation.

4.2. Overexpression of Ubiquitin-Specific Protease 7 Promotes Hepatocellular Carcinoma Cell Migration, Invasion, and Epithelial-Mesenchymal Transition

We explored the impact of USP7 expression on the malignant biological behaviors of HCC cells. Transwell assay revealed that HCC cells transfected with OE-USP7 had markedly increased migrating and invading cell numbers, while cells transfected with sh-USP7 had notably decreased cell numbers (Figure 2A and B). A significant attenuation of E-cadherin fluorescence and enhancement of Vimentin signal were observed in HCC cells transfected with OE-USP7. In contrast, cells transfected with sh-USP7 exhibited enhanced E-cadherin fluorescence signaling and diminished Vimentin fluorescence intensity, suggesting that USP7 regulates the EMT process in HCC cells (Figure 2C and D). Not only that, overexpression of USP7 markedly reduced E-cadherin protein level in HCC cells, while upregulating N-cadherin, Vimentin, and Snail; whereas knockdown of USP7 caused elevated E-cadherin level and significant downregulation of Vimentin, N-cadherin, and Snail (Figure 2E-I). Together, these results suggest that USP7 enhances the migration and invasion of HCC cells while also promoting the EMT process of HCC cells.

4.3. Overexpression of Ubiquitin-Specific Protease 7 Promotes Cancer Stem Cells -Like Properties in Hepatocellular Carcinoma

It has been reported that there is upregulation of characteristic stemness markers (e.g., CD44, CD133, CD24, CD90, EpCAM, etc.) in CSCs (34, 35). Flow cytometry analysis revealed that Huh-7 cells exhibited a notably greater proportion of cells co-expressing CD44 and CD133 compared to HCCLM3 cells, suggesting that Huh-7 cells have stronger stem cell properties (Figure 3A). Based on this characterization difference, Huh-7 cells were selected as a model for subsequent functional validation. The impact of USP7 on the sphere-forming ability was tested by examining the efficiency of cell

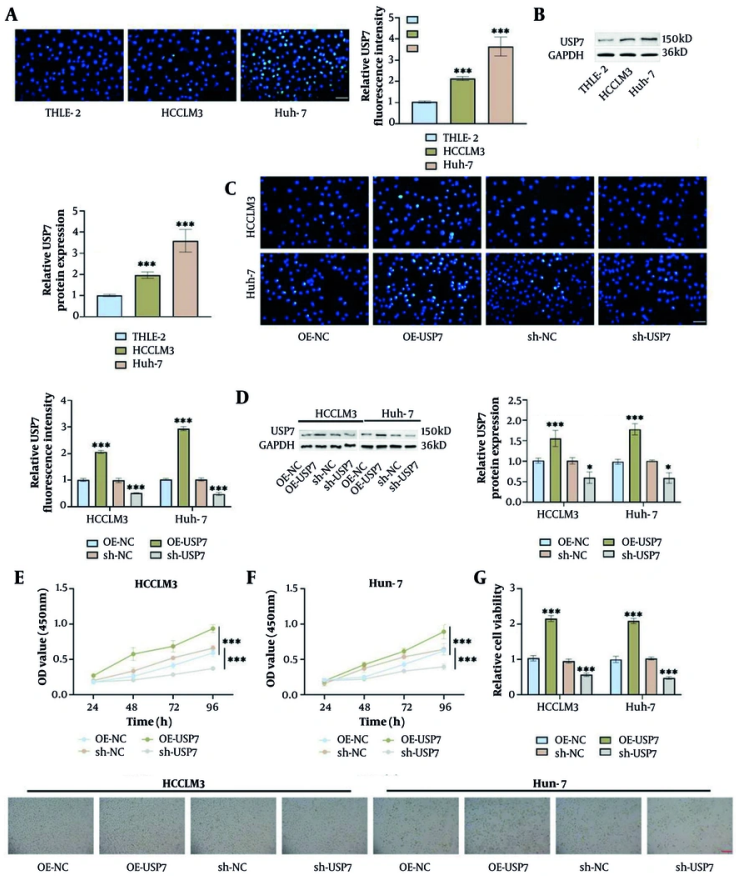

Figure 1. Ubiquitin-specific protease 7 (USP7) is elevated in hepatocellular carcinoma (HCC) and overexpression of USP7 promotes HCC cell proliferation. A, immunofluorescence results confirmed that USP7 expression was higher in HCC cell lines (HCCLM3 and Huh-7) than in normal cells (THLE-2) (40×, 50 µm). B, USP7 level in HCC cell lines was higher than in THLE-2 cells as measured via Western blot. C, immunofluorescence assays confirmed that transfection of OE-USP7 in HCC cells resulted in an increased USP7 level, whereas sh-USP7 caused a decreased USP7 level (40×, 50 µm). D, Western blot analysis indicated that transfection of OE-USP7 elevated USP7 level in HCC cells, while transfection of sh-USP7 resulted in decreased USP7 levels. E-F, cell counting kit-8 (CCK-8) assay showed that transfection of OE-USP7 resulted in increased proliferative capacity of HCC cells, while transfection of sh-USP7 resulted in decreased proliferative capacity. G, cell microscopic images revealed that cell viability was elevated by transfection with OE-USP7 and decreased by transfection with sh-USP7 (10×, 200 µm), (n = 3, * $P < 0.05$, *** $P < 0.001$).

sphere formation of tumor cells in conditioned media. The results showed that Huh-7 cells transfected with OE-USP7 formed significantly more tumor spheres with larger sphere diameters, while cells transfected with sh-USP7 had significantly reduced sphere-forming ability and formed spheres with smaller diameters (Figure 3B). Overexpression of USP7 caused a marked upregulation of CD44 and CD133 protein levels, whereas knockdown of USP7 caused a notable decline in their protein levels (Figure 3C-E). Additionally, overexpression of USP7 markedly elevated stemness factors C-Myc, SOX2, OCT4, Nanog, and KLF4 levels in Huh-7 cells. But knockdown of USP7 caused a notable downregulation of protein expression of the aforementioned stemness factors (Figure 3F-K). These findings revealed a positive relationship between the levels of USP7 expression and the characteristics associated with CSCs-like properties of HCC cells, and overexpression of USP7 enhanced these CSCs-like properties, whereas knockdown of USP7 inhibited their stemness.

4.4. Inhibition of Malignant Biological Processes in Hepatocellular Carcinoma by Ubiquitin-Specific Protease 7 via the AKT/β-Catenin Pathway

To investigate how USP7 facilitates the aggressive advancement of HCC, we assessed the associated signaling pathways. Overexpression of USP7 notably

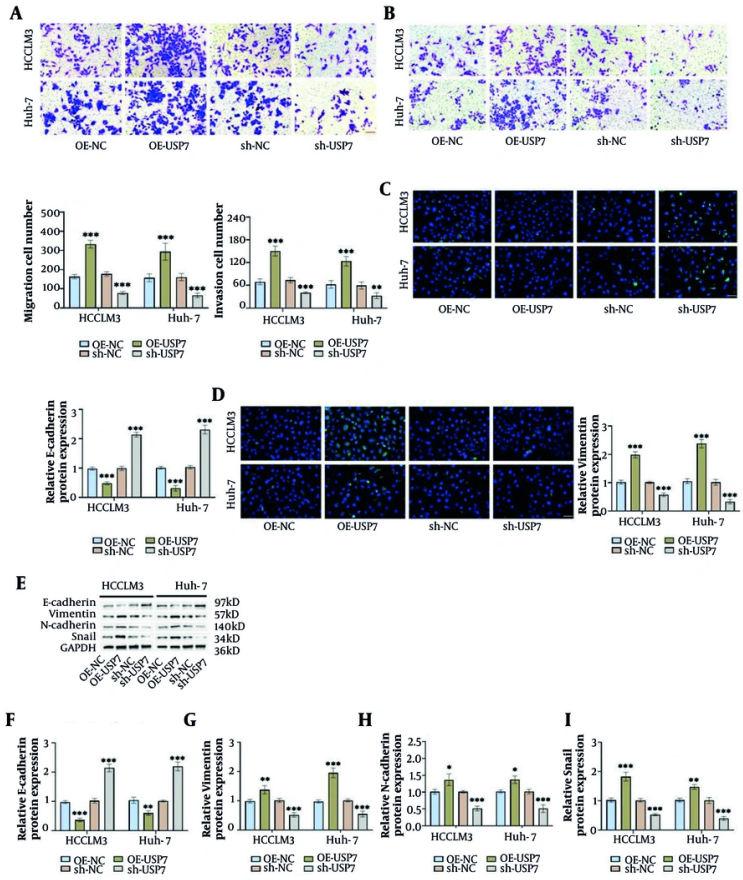

Figure 2. Overexpression of ubiquitin-Specific Protease 7 (USP7) enhances migration, invasion, and epithelial-mesenchymal transition (EMT) in hepatocellular carcinoma (HCC) cells. A and B, Transwell assay confirmed that transfection of OE-USP7 boosted the number of migrating and invading cells, while transfection of sh-USP7 diminished these cell counts (20×, 100 μm). C and D, immunofluorescence demonstrated a decline in E-cadherin fluorescence intensity and a rise in Vimentin level in HCC cells after transfection with OE-USP7, and transfection with sh-USP7 had the opposite effect to that of transfection with OE-USP7 (40×, 50 μm). E-I, Western blot demonstrated that overexpression of USP7 declined E-cadherin level and increased Vimentin, N-cadherin, and Snail levels, whereas silencing USP7 had the opposite effect of overexpression of USP7 (n = 3, * $P < 0.05$, ** $P < 0.01$, *** $P < 0.001$).

upregulated β-catenin level and promoted AKT and GSK3β phosphorylation in Huh-7 cells. In contrast, silencing of USP7 caused a marked reduction in the activation levels of the above pathway-related proteins (Figure 4A-D). PI3K serves as an upstream regulator of the AKT/β-catenin pathway (36). To verify whether USP7 exerts its effects via this pathway, we intervened using the PI3K inhibitor LY294002 and activator 740Y-P. LY294002 treatment markedly attenuated the elevated levels of β-catenin, p-AKT/AKT, and p-GSK3β/GSK3β induced by overexpression of USP7, whereas 740Y-P treatment further increased the expression levels of the above proteins (Figure 4E-H). After overexpression of USP7, the proliferative ability of Huh-7 cells was significantly enhanced, and LY294002 markedly weakened the proliferative ability; whereas 740Y-P further enhanced the proliferative ability (Figure 4I). Huh-7 cells transfected with OE-USP7 showed a typical proliferatively active phenotype with tight cell apposition and full morphology; after LY294002 intervention, the cells appeared to be wrinkled and had a decreased apposition capacity; whereas 740Y-P treatment resulted in a fuller morphology and tight cell apposition (Figure 4J). In addition, overexpression of USP7 markedly boosted the migrating and invading number in Huh-7 cells. LY294002 intervention reversed this effect with a significant reduction in migrating and invading cells; whereas 740Y-P treatment synergized with USP7 to further increase migrating and invading cell numbers (Figure 4K-L). Notably, LY294002

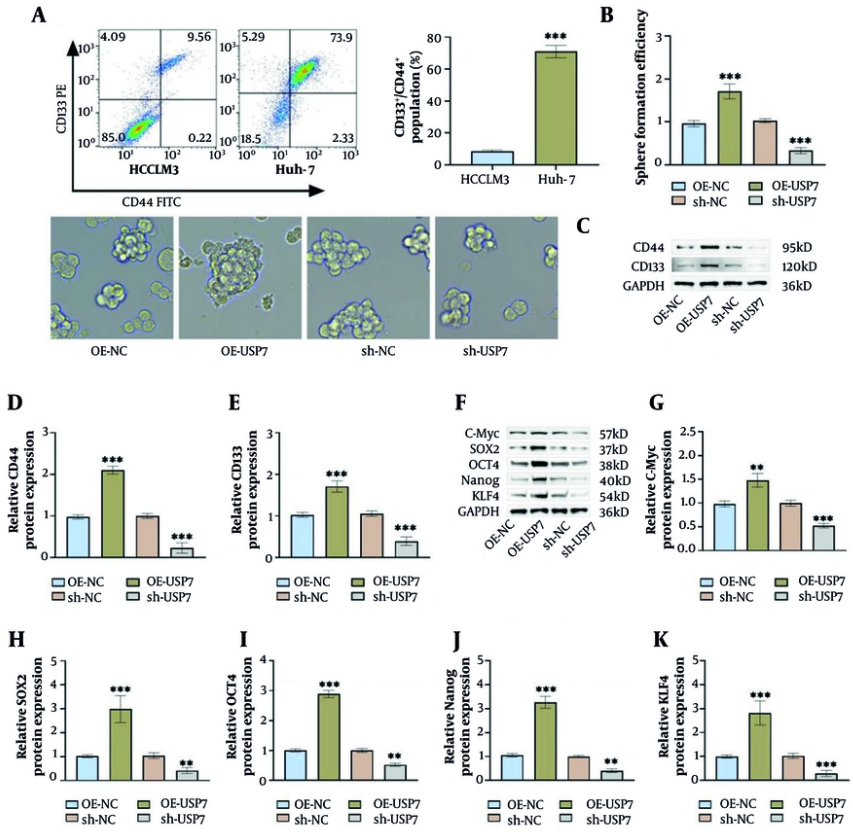

Figure 3. Overexpression of ubiquitin-specific protease 7 (USP7) promotes cancer stem cells (CSCs)-like properties in hepatocellular carcinoma (HCC). A, flow cytometry assay indicated that the proportion of CD44+CD133+ cells in Huh-7 cells was greater than that in HCCLM3 cells, so Huh-7 cells were selected for the follow-up study. B, Sphere formation assay showed that transfection of OE-USP7 increased the spheroplast ability of Huh-7 cells, while transfection of sh-USP7 decreased the spheroplast ability. C-E, overexpression of USP7 increased CD44 and CD133 levels in CSCs as measured by Western blot, and silencing of USP7 decreased CD44 and CD133 levels. F-K, overexpression of USP7 increased C-Myc, SOX2, OCT4, Nanog, and KLF4 protein levels as examined by Western blot, and silencing of USP7 decreased the expression levels of these tumor stemness factors (n = 3, ** P < 0.01, *** P < 0.001).

intervention attenuated the effect of OE-USP7, leading to an increase in E-cadherin levels while simultaneously decreasing Vimentin, N-cadherin, and Snail levels; whereas 740Y-P treatment enhanced the effect of overexpressed USP7 (Figure 4M-Q). The above results confirm that USP7 stimulates the AKT/β-catenin pathway, subsequently triggering the EMT process, whereas blocking or activating the AKT/β-catenin pathway reverses or enhances this process accordingly.

4.5. Ubiquitin-Specific Protease 7 Promotes Cancer Stem Cells-Like Properties in Hepatocellular Carcinoma Through Modulating the AKT/β-Catenin Pathway

Next, we explored whether USP7 promotes CSCs-like characteristics in HCC cells through modulating the AKT/β-catenin pathway. The number and diameter of tumor spheres formed by Huh-7 cells transfected with OE-USP7 were increased. When LY294002 was added, the OE-USP7-induced sphere-forming effect was weakened; whereas, 740Y-P treatment enhanced the effect of OE-USP7, resulting in further enhancement of the number and diameter of tumor spheres (Figure 5A). Overexpression of USP7 markedly up-regulated CD44 and CD133 protein levels in Huh-7 cells, which were significantly reduced by LY294002 intervention; while 740Y-P treatment further enhanced the up-regulatory effect of overexpression of USP7 on CD44 and CD133 (Figure 5B-D). Additionally, overexpression of USP7 notably increased the stemness factors C-Myc, SOX2, OCT4, Nanog, and KLF4 levels. The above-mentioned stemness factors levels were markedly decreased after LY294002 intervention, while 740Y-P treatment

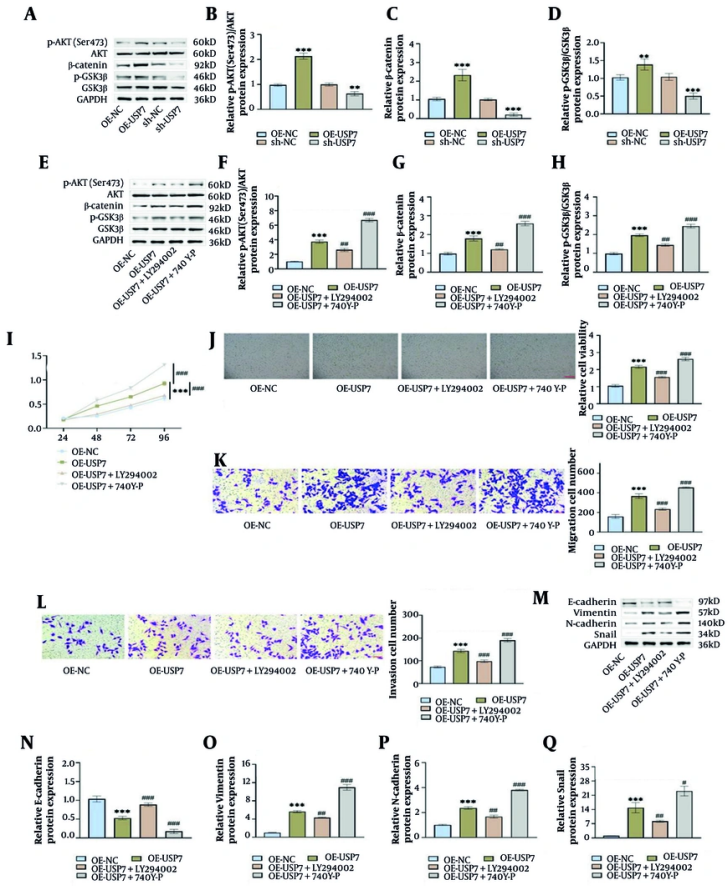

Figure 4. Ubiquitin-specific protease 7 (USP7) can inhibit the malignant biological process of hepatocellular carcinoma (HCC) cells via regulating the AKT/β-catenin pathway. A-D, overexpression of USP7 elevated p-AKT (Ser473)/AKT, β-catenin, and p-GSK3β/GSK3β levels in Huh-7 cells as examined by Western blot, and silencing of USP7 decreased these AKT/β-catenin pathway-related protein levels. E-H, Western blot measured that the PI3K inhibitor LY294002 attenuated the impact of OE-USP7, resulting in reduced p-AKT (Ser473)/AKT, β-catenin, and p-GSK3β/GSK3β levels, whereas the PI3K activator 740Y-P exerted the opposite effect. I, cell counting kit-8 (CCK-8) assay showed that transfection of OE-USP7 resulted in increased proliferative capacity of Huh-7 cells, whereas LY294002 weakened the impact of OE-USP7, but 740Y-P further increased the cell proliferation capacity. J, cell microscopic images showed increased cell viability after transfection with OE-USP7, and LY294002 intervention weakened the effect of OE-USP7, but 740Y-P further increased cell viability (10×, 200 μm). K-L, Transwell assay indicated that overexpression of USP7 increased the migrating and invading cell numbers, and LY294002 intervention declined these cell numbers, but 740Y-P treatment improved the effect of overexpression of USP7 (20×, 100 μm). M-Q, Western blot measured that LY294002 weakened the effect of OE-USP7, causing increased E-cadherin level and decreased Vimentin, N-cadherin, and Snail levels, whereas 740Y-P treatment had the opposite effect to LY294002 (n = 3, ** P < 0.01, *** P < 0.001 vs OE-NC, # P < 0.05, ## P < 0.01, ### P < 0.001 vs OE-USP7).

synergized with OE-USP7 to further enhance the expression levels of these stemness factors (Figure 5E-J). The findings indicate that USP7's influence on the stemness of HCC cells might be contingent upon the activation of the AKT/β-catenin pathway.

4.6. Knockdown of Ubiquitin-Specific Protease 7 Inhibits AKT/β-Catenin Pathway Activation and Suppresses Tumor Growth and Cancer Stem Cells-Like Properties

By subcutaneous injection of Huh-7 cells, we constructed an HCC tumor model in nude mice to explore the impact of USP7 on tumor growth and CSCs-like properties in vivo. Injection of Huh-7 cells transfected with sh-USP7 significantly reduced USP7 protein levels, accompanied by a marked downregulation of AKT/β-catenin pathway-related proteins. In contrast, USP7 protein level was notably elevated after transfection with OE-USP7, and the activation levels of the above pathway molecules were similarly elevated (Figure 6A-E). In vivo tumors in nude mice in the sh-USP7 group were significantly reduced in volume and weight, while the OE-USP7 group showed a marked rise in tumor size and mass (Figure 6F-H). Next,

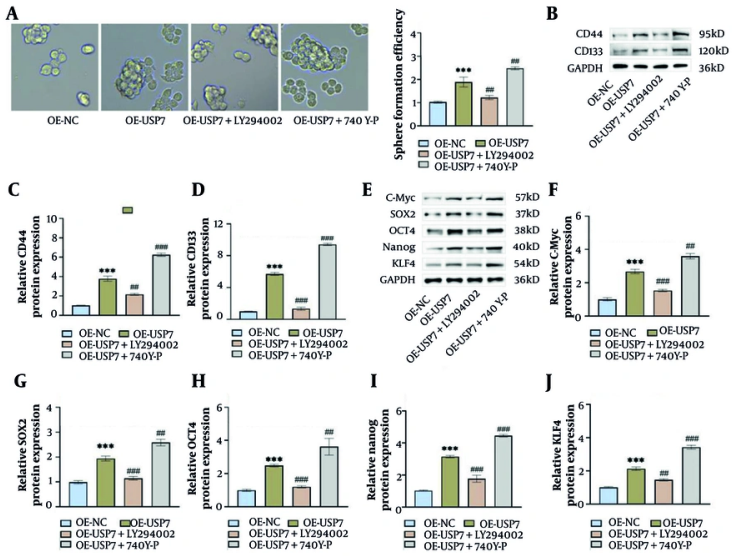

Figure 5. Ubiquitin-specific protease 7 (USP7) promotes cancer stem cells (CSCs)-like properties in hepatocellular carcinoma (HCC) by modulating the AKT/β-catenin pathway. A, Sphere formation assay showed that transfection of OE-USP7 improved the spheroplast ability of Huh-7 cells, but LY294002 treatment weakened the effect of OE-USP7, whereas 740Y-P improved the effect of OE-USP7. B-D, overexpression of USP7 raised CD44 and CD133 levels in CSCs as measured by Western blot, and LY294002 intervention resulted in decreased levels of CD44 and CD133, whereas 740Y-P increased the effect of OE-USP7. E-J, overexpression of USP7 increased C-Myc, SOX2, OCT4, Nanog, and KLF4 levels as examined by Western blot, and LY294002 intervention resulted in decreased levels of expression of tumor stemness factors, whereas 740Y-P treatment increased the effect of OE-USP7 (n = 3, *** P < 0.001 vs OE-NC, ## P < 0.01, ### P < 0.001 vs OE-USP7).

the positivity of the proliferation marker Ki67 in tumor tissues was detected by immunohistochemistry. Ki-67 positivity was notably decreased in the sh-USP7 group, with brownish-yellow stained cells scattered; Ki-67-positive cells were densely packed and staining intensity was enhanced in the OE-USP7 group, suggesting that knockdown of USP7 could inhibit tumor growth (Figure 6I). Additionally, knockdown of USP7 markedly up-regulated E-cadherin level in tumor tissues, while decreasing Vimentin, N-cadherin, and Snail levels, suggesting that the EMT process was blocked. Cancer stem cells markers CD133 and CD44 and stemness transcription factors C-Myc, SOX2, OCT4, Nanog, and KLF4 levels were likewise significantly downregulated with USP7 knockdown. On the contrary, tumor tissues overexpressing USP7 showed reduced E-cadherin expression and elevated mesenchymal markers and stemness factors (Figure 6J-M). These results suggest that knockdown of USP7 inhibits malignant progression of HCC in vivo through blocking the AKT/β-catenin pathway to suppress the EMT process and inhibit CSCs properties.

5. Discussion

Hepatocellular carcinoma ranks among the most aggressive tumors with complex and heterogeneous pathogenic causes, and despite the widespread use of surgical and chemoradiotherapy treatments, the five-year survival rate for HCC patients is still low, a situation that highlights the urgency of developing novel treatment strategies (7, 37). Therefore, the search for molecular targets for the treatment of HCC could help to prolong patient survival and increase the cure rate. Ubiquitin-specific protease 7, a significant player in the deubiquitinating enzyme family, is considered a key cancer target (17). Our prior investigations revealed that USP7 boosts the stemness of HCC cells and contributes to HCC malignant progression (21). This research investigated USP7 level in HCC cell lines and normal hepatocytes and revealed that USP7 was abnormally highly expressed in HCC, aligning with the findings of Ying et al. (20). In cell function studies, overexpression of USP7 promoted HCC cell proliferation, increased cell viability, and facilitated migration and invasion. In contrast, knockdown of USP7 markedly suppressed these malignant biological behaviors. The in vivo experiments also confirmed that knockdown of USP7 inhibited HCC tumor growth and CSCs characteristics, implying that USP7 could serve as a significant target for

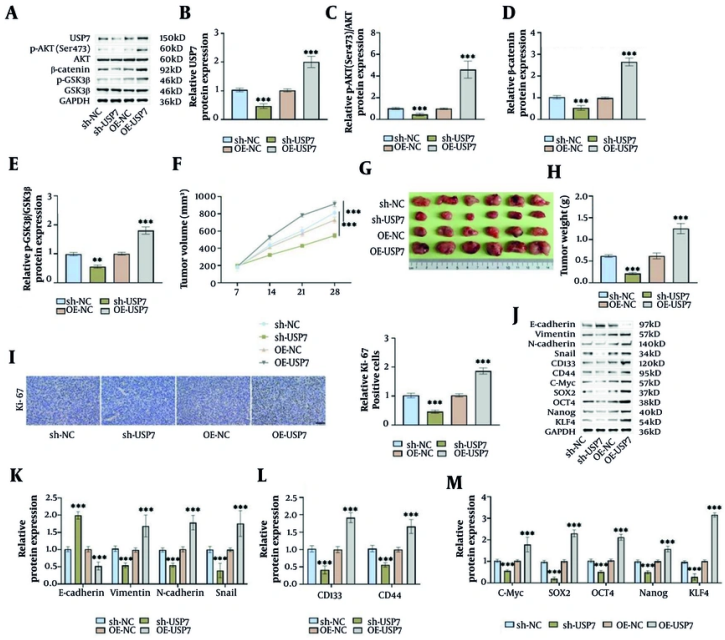

Figure 6. Knockdown of ubiquitin-specific protease 7 (USP7) hinders the AKT/β-catenin pathway and suppresses tumor growth and cancer stem cells (CSCs)-like properties. A-E, Western blot examined that injection of Huh-7 cells transfected with sh-USP7 resulted in decreased levels of USP7 in tumor tissues, as well as decreased p-AKT (Ser473)/AKT, β-catenin, and p-GSK3β/GSK3β levels, whereas transfection of OE-USP7 resulted in increased USP7 and AKT/β-catenin pathway-associated protein levels. F-H, the size of subcutaneous tumors in nude mice was examined weekly by vernier calipers. On the 28th day, the tumors were isolated, photographed for documentation, and weighed. I, immunohistochemistry measured that silencing USP7 effectively reduced Ki-67 levels, while overexpression of USP7 increased Ki-67 levels (40×, 50 μm). J-M, silencing USP7 caused an increased E-cadherin level and decreased Vimentin, N-cadherin, Snail, CD133, CD44, C-Myc, SOX2, OCT4, Nanog, and KLF4 levels in the tumor tissues as measured by Western blot, whereas transfection of OE-USP7 had the opposite effect (n = 6, ** P < 0.01, *** P < 0.001).

treating HCC. It is worth noting that the subcutaneous xenograft model may not be able to effectively evaluate the invasion and metastasis of tumors. However, this study focuses on the regulatory effect of USP7 on the growth of HCC tumors. In the future, the regulatory effect of USP7 on the invasion and metastasis of HCC can be further explored through in situ liver tumor models.

EMT refers to the biological process during which epithelial cells lose their cellular polarity and intercellular adhesion, while acquiring the migratory and invasive characteristics of mesenchymal cells (38, 39). This process is crucial for embryonic development and tissue repair but is aberrantly activated in tumors, serving as a primary factor in the central driving mechanisms of malignant metastasis and treatment resistance (40). Epithelial-mesenchymal transitionis primarily characterized by an increase in mesenchymal markers (e.g., Vimentin and N-cadherin), a decline in the epithelial marker E-cadherin, and activation of EMT transcription factors like Snail, which drives the epithelial-to-mesenchymal phenotypic transition (41). N-cadherin overexpression promotes tumor cell invasion and migration, whereas deficient E-cadherin level reduces the stability of epithelial cell-cell adhesion junctions, thereby promoting tumor cell metastasis. Our research revealed that increasing the levels of USP7 caused a reduction of E-cadherin level while simultaneously elevating Vimentin, N-cadherin, and Snail levels; whereas knockdown of USP7 led to the opposite result, suggesting that USP7 is a positive regulator of the EMT process. This mechanism is similar to the recently reported mode of action of USP7 in non-small cell lung cancer, where GNE-6776 (USP7 inhibitor) triggers apoptosis in tumor cells through inhibiting the EMT process and decreasing the mitochondrial membrane potential (42). In addition, Bian et al. found that Flap endonuclease 1 upregulated USP7, and the former-mediated proliferation and EMT process in HCC cells could be significantly reversed by the USP7 inhibitor P22077 (43). The findings indicate that USP7 may ultimately promote HCC progression by promoting EMT, leading to increased cell invasion and metastasis.

Cancer stem cells (CSCs) are a subset of undifferentiated cells in tumor tissues with self-renewal ability and the ability to generate heterogeneous tumors, which are strongly linked to tumor proliferation, metastasis, and recurrence (44, 45). In other words, tumorigenesis, progression, and metastasis are essentially the process of accumulating heterogeneity of CSCs. It has been demonstrated that CSCs exhibit upregulated levels of characteristic markers, such as CD24, CD44, CD133, EpCAM, etc., and that all of these stemness markers with upregulated expression are associated with progressive HCC and poorer patient prognosis (34, 35, 46). In addition, CD133 is also likely to be an important contributor to the heterogeneity of HCC production (47). Cancer stem cells transcription factors, including KLF4, SOX2, OCT4, c-MYC, and Nanog, are critical regulatory genes that maintain the multipotential properties and self-renewal capacity of stem cells (48-50). Notably, the properties of CSCs in tumor cells are closely related to the EMT process (51). In this study, Huh-7 cells had a higher proportion of CD44+CD133+ double-positively expressing cells, suggesting stronger CSCs-like properties. Not only that, overexpression of USP7 enhanced the cell-forming ability of Huh-7 cells and upregulated the protein levels of CD44 and CD133, with increased C-Myc, SOX2, OCT4, Nanog, and KLF4 protein levels. Whereas knockdown of USP7 led to the opposite result, this finding builds upon the earlier conclusion that USP7 enhances HCC stemness, further clarifying USP7's regulatory role in CSC core markers and regulatory factors.

Glycogen synthase kinase-3β is a type of serine/threonine kinase isoform that plays an important role in numerous biological functions, like apoptosis, DNA repair, cell cycle, tumor growth, and tumor immunity (52). Glycogen synthase kinase-3β could be regulated by several signaling pathways, of which the AKT/β-catenin pathway is one of the major ones (53, 54). The classical activation pattern of this pathway is that growth factors (e.g., HGF, IGF-1) bind to membrane surface receptors, trigger the activation of the PI3K catalytic subunit, recruit AKT to the cell membrane and phosphorylate it for activation. Activated AKT inactivates GSK3β by phosphorylating it, which causes β-catenin to accumulate in the cytoplasm and eventually move into the nucleus, initiating the transcription of EMT-related genes and genes that maintain CSCs-like properties (55-57). Based on the importance of AKT/β-catenin in the CSCs-like properties and EMT process of tumor cells, we explored whether USP7 promotes HCC progression by regulating this pathway. A report indicated that USP7 promotes Wnt/β-catenin pathway activation by enhancing the stability of the RNA deconjugating enzyme DD3X protein, playing a critical role in the partial EMT status, invasion, and metastasis of colorectal cancer cells (58). Additionally, USP7 deubiquitinates and enhances the stability of β-catenin, thereby promoting malignant progression in colorectal cancer (59). In this study, overexpression of USP7 upregulated β-catenin level and promoted AKT and GSK3β phosphorylation in Huh-7 cells. In contrast, silencing of USP7 hindered the activation of the above pathway-associated proteins, suggesting that USP7 regulates the AKT/β-catenin pathway. Importantly, treatment with the PI3K inhibitor LY294002 attenuated the CSCs-like properties and EMT process induced by overexpression of USP7, whereas the activator 740Y-P further promoted the effect of overexpression of USP7. In addition, USP7 also modulates the AKT/β-catenin pathway in mice, and knockdown of USP7 inhibits tumor growth and CSCs-like properties, whereas overexpression of USP7 does the opposite. These results confirm that USP7 may promote the CSCs-like characteristics and EMT process of HCC cells by modulating the AKT/β-catenin pathway, thereby promoting malignant tumor progression.

This study has certain limitations that must be objectively acknowledged. Although both in vitro and in vivo experiments have confirmed the role of USP7, the lack of validation of clinical specimens and the correlation between the expression level of USP7 and the clinicopathological features (e.g., tumor stage, metastatic status, and prognosis) of patients with HCC still need to be further clarified. In the future, the interaction between USP7 and the key molecules of the AKT/β-catenin pathway can be directly verified through techniques such as Co-IP and ubiquitination experiments, in order to further clarify the complete mechanism by which USP7 regulates the oncogenic function of β-catenin. Furthermore, in different cancer cells, USP7 may regulate the AKT signaling pathway through distinct mechanisms. Future studies could investigate the specific ways USP7 modulates the AKT signaling pathway in various cancer cell types.

5.1. Conclusions

Ubiquitin-specific protease 7 enhances the aggressive characteristics of tumors and promotes the CSCs properties and EMT process in HCC cells by activating the AKT/β-catenin pathway. Inhibition of USP7 inhibited HCC progression by blocking this pathway, indicating that USP7 may be a valuable target for treatment strategies aimed at HCC metastasis and stemness. This investigation revealed the mechanism of action of USP7

in promoting the malignant progression of HCC and expanded the tumor biological functions of USP7. In the future, the interaction between the USP7-activated AKT/β-catenin pathway and other pathways could be explored to further clarify its mechanism of action. Meanwhile, it is necessary to expand the sample size in subsequent studies to enhance the reliability and generalizability of the findings and to provide a more solid theoretical basis for therapeutic research on HCC.

Footnotes

AI Use Disclosure: The authors declare that no generative AI tools were used in the creation of this article.

Authors' Contribution: M. H. and X. J.: Edited and refined the manuscript with a focus on critical intellectual contributions. Y. Z., L. W., and H. Y.: Participated in collecting, assessing, and interpreting the data. Made significant contributions to data interpretation and manuscript preparation. R. X., J. Z., and L. Y.: Developed and planned the study, performed experiments, and interpreted results. Mi. H.: Provided substantial intellectual input during the drafting and revision of the manuscript. The final version of the manuscript has been reviewed and approved by all authors.

Conflict of Interests Statement: The authors declare that they have no financial conflicts of interest.

Data Availability: The dataset presented in the study is available on request from the corresponding author during submission or after its publication. The data are not publicly available due to privacy.

Ethical Approval: This study is approved by the Ethics Committee of the Sheyang People's Hospital under the ethical approval code of 2024128.

Funding/Support: This research did not receive any external funding support.

References

1. McGlynn KA, Petrick JL, Groopman JD. Liver Cancer: Progress and Priorities. *Cancer Epidemiol Biomarkers Prev*. 2024;**33**(10):1261-72. [PubMed ID: 39354815]. https://doi.org/10.1158/1055-9965.EPI-24-0686.
2. Siegel RL, Kratzer TB, Giaquinto AN, Sung H, Jemal A. Cancer statistics, 2025. *CA Cancer J Clin*. 2025;**75**(1):10-45. [PubMed ID: 39817679]. [PubMed Central ID: PMC11745215]. https://doi.org/10.3322/caac.21871.
3. Zheng J, Wang S, Xia L, Sun Z, Chan KM, Bernards R, et al. Hepatocellular carcinoma: signaling pathways and therapeutic advances. *Signal Transduct Target Ther*. 2025;**10**(1):35. [PubMed ID: 39915447]. [PubMed Central ID: PMC11802921]. https://doi.org/10.1038/s41392-024-02075-w.
4. Lim RY, Koh B, Ng CH, Kulkarni AV, Liu K, Wijarnpreecha K, et al. Hepatocellular Carcinoma Surveillance and Survival in a Contemporary Asia-Pacific Cohort. *JAMA Netw Open*. 2025;**8**(7). e2520294. [PubMed ID: 40643909]. [PubMed Central ID: PMC12254890]. https://doi.org/10.1001/jamanetworkopen.2025.20294.
5. Fuster-Anglada C, Mauro E, Ferrer-Fabrega J, Caballol B, Sanduzzi-Zamparelli M, Bruix J, et al. Histological predictors of aggressive recurrence of hepatocellular carcinoma after liver resection. *J Hepatol*. 2024;**81**(6):995-1004. [PubMed ID: 38925272]. https://doi.org/10.1016/j.jhep.2024.06.018.
6. Chidambaranathan-Reghupaty SP, Sarkar D. Hepatocellular carcinoma (HCC): Epidemiology, etiology and molecular classification. In: Sarkar D, Fisher PB, editors. *Mechanisms and Therapy of Liver Cancer*. Cambridge, United Kingdom: Academic Press; 2021. p. 1-61. https://doi.org/10.1016/bs.acr.2020.10.001.
7. Ganesan P, Kulik LM. Hepatocellular Carcinoma: New Developments. *Clin Liver Dis*. 2023;**27**(1):85-102. [PubMed ID: 36400469]. https://doi.org/10.1016/j.cld.2022.08.004.
8. Wang X, Lu J. Immunotherapy for hepatocellular carcinoma. *Chin Med J*. 2024;**137**(15):1765-76. [PubMed ID: 38855876]. [PubMed Central ID: PMC12077568]. https://doi.org/10.1097/CM9.0000000000003060.
9. Fang X, Yan Q, Liu S, Guan XY. Cancer Stem Cells in Hepatocellular Carcinoma: Intrinsic and Extrinsic Molecular Mechanisms in Stemness Regulation. *Int J Mol Sci*. 2022;**23**(20). [PubMed ID: 36293184]. [PubMed Central ID: PMC9604119]. https://doi.org/10.3390/ijms232012327.
10. Niu Q, Ye S, Zhao L, Qian Y, Liu F. The role of liver cancer stem cells in hepatocellular carcinoma metastasis. *Cancer Biol Ther*. 2024;**25**(1):2321768. [PubMed ID: 38393655]. [PubMed Central ID: PMC10896152]. https://doi.org/10.1080/15384047.2024.2321768.
11. Chen S, Du Y, Guan XY, Yan Q. The current status of tumor microenvironment and cancer stem cells in sorafenib resistance of hepatocellular carcinoma. *Front Oncol*. 2023;**13**:1204513. [PubMed ID: 37576900]. [PubMed Central ID: PMC10412930]. https://doi.org/10.3389/fonc.2023.1204513.
12. Zhang M, Wei T, Guo D. The role of abnormal ubiquitination in hepatocellular carcinoma pathology. *Cell Signal*. 2024;**114**:110994. [PubMed ID: 38036196]. https://doi.org/10.1016/j.cellsig.2023.110994.
13. Hu X, Chen G, Huang Y, Cheng Q, Zhuo J, Su R, et al. Integrated Multiomics Reveals Silencing of has_circ_0006646 Promotes TRIM21-Mediated NCL Ubiquitination to Inhibit Hepatocellular Carcinoma Metastasis. *Adv Sci*. 2024;**11**(16). e2306915. [PubMed ID: 38357830]. [PubMed Central ID: PMC11040345]. https://doi.org/10.1002/advs.202306915.
14. Wang X, Li Y, Li Y, Liu P, Liu S, Pan Y. FBXW7 Reduces the Cancer Stem Cell-Like Properties of Hepatocellular Carcinoma by Regulating the Ubiquitination and Degradation of ACTL6A. *Stem Cells Int*. 2022;**2022**:3242482. [PubMed ID: 36159747]. [PubMed Central ID: PMC9492413]. https://doi.org/10.1155/2022/3242482.
15. Al-Eidan A, Wang Y, Skipp P, Ewing RM. The USP7 protein interaction network and its roles in tumorigenesis. *Genes Dis*. 2022;**9**(1):41-50. [PubMed ID: 35005106]. [PubMed Central ID: PMC8720671]. https://doi.org/10.1016/j.gendis.2020.10.004.
16. Dai X, Lu L, Deng S, Meng J, Wan C, Huang J, et al. USP7 targeting modulates anti-tumor immune response by reprogramming Tumor-associated Macrophages in Lung Cancer. *Theranostics*. 2020;**10**(20):9332-47. [PubMed ID: 32802195]. [PubMed Central ID: PMC7415808]. https://doi.org/10.7150/thno.47137.
17. Saha G, Roy S, Basu M, Ghosh MK. USP7 - a crucial regulator of cancer hallmarks. *Biochim Biophys Acta Rev Cancer*. 2023;**1878**(3):188903.

[PubMed ID: 37127084]. https://doi.org/10.1016/j.bbcan.2023.188903.

18. Carreira LD, Oliveira RI, Moreira VM, Salvador JAR. Ubiquitin-specific protease 7 (USP7): an emerging drug target for cancer treatment. *Expert Opin Ther Targets*. 2023;**27**(11):1043-58. [PubMed ID: 37789645]. https://doi.org/10.1080/14728222.2023.2266571.
19. Korenev G, Yakukhnov S, Druk A, Golovina A, Chasov V, Mirgayazova R, et al. USP7 Inhibitors in Cancer Immunotherapy: Current Status and Perspective. *Cancers*. 2022;**14**(22). [PubMed ID: 36428632]. [PubMed Central ID: PMC9688046]. https://doi.org/10.3390/cancers14225539.
20. Ying H, Zhang B, Cao G, Wang Y, Zhang X. Role for ubiquitin-specific protease 7 (USP7) in the treatment and the immune response to hepatocellular carcinoma: potential mechanisms. *Transl Cancer Res*. 2023;**12**(11):3016-33. [PubMed ID: 38130306]. [PubMed Central ID: PMC10731377]. https://doi.org/10.21037/tcr-23-153.
21. Hu M, Dai C, Sun X, Chen Y, Xu N, Lin Z, et al. Ubiquitination-specific protease 7 enhances stemness of hepatocellular carcinoma by stabilizing basic transcription factor 3. *Funct Integr Genomics*. 2024;**24**(1):28. [PubMed ID: 38340226]. https://doi.org/10.1007/s10142-024-01310-5.
22. Zhu Z, Cao C, Zhang D, Zhang Z, Liu L, Wu D, et al. UBE2T-mediated Akt ubiquitination and Akt/beta-catenin activation promotes hepatocellular carcinoma development by increasing pyrimidine metabolism. *Cell Death Dis*. 2022;**13**(2):154. [PubMed ID: 35169125]. [PubMed Central ID: PMC8847552]. https://doi.org/10.1038/s41419-022-04596-0.
23. Cao L, Weng K, Li L, Lin G, Zhao Y, Gao Y, et al. BATF2 inhibits the stem cell-like properties and chemoresistance of gastric cancer cells through PTEN/AKT/beta-catenin pathway. *Theranostics*. 2024;**14**(18):7007-22. [PubMed ID: 39629124]. [PubMed Central ID: PMC11610130]. https://doi.org/10.7150/thno.98389.
24. Chan XY, Chang KP, Yang CY, Liu CR, Hung CM, Huang CC, et al. Upregulation of ENAH by a PI3K/AKT/beta-catenin cascade promotes oral cancer cell migration and growth via an ITGB5/Src axis. *Cell Mol Biol Lett*. 2024;**29**(1):136. [PubMed ID: 39511483]. [PubMed Central ID: PMC11545229]. https://doi.org/10.1186/s11658-024-00651-0.
25. Yang Z, Zhang P, Zhao Y, Guo R, Hu J, Wang Q, et al. DRD4 promotes chemo-resistance and cancer stem cell-like phenotypes by mediating the activation of the Akt/beta-catenin signaling axis in liver cancer. *Br J Cancer*. 2024;**131**(7):1212-23. [PubMed ID: 39174739]. [PubMed Central ID: PMC11442912]. https://doi.org/10.1038/s41416-024-02811-7.
26. Guo W, Liu M, Luo W, Peng J, Liu F, Ma X, et al. FERMT1 promotes epithelial-mesenchymal transition of hepatocellular carcinoma by activating EGFR/AKT/beta-catenin and EGFR/ERK pathways. *Transl Oncol*. 2024;**50**:102144. [PubMed ID: 39353234]. [PubMed Central ID: PMC11472111]. https://doi.org/10.1016/j.tranon.2024.102144.
27. Karimi S, Ahmadpour F, Mohammadi M. Assessing the Protective Role of Wharton's Jelly-Derived Mesenchymal Stem Cell Secretomes in Inducing Apoptosis in SKBR3 Breast Carcinoma Cells. *Jentashapir J Cell Mol Biol*. 2025;**16**(1). https://doi.org/10.5812/jjcmb-157354.
28. Zhong Y, Yu F, Yang L, Wang Y, Liu L, Jia C, et al. HOXD9/miR-451a/PSMB8 axis is implicated in the regulation of cell proliferation and metastasis via PI3K/AKT signaling pathway in human anaplastic thyroid carcinoma. *J Transl Med*. 2023;**21**(1):817. [PubMed ID: 37974228]. [PubMed Central ID: PMC10652604]. https://doi.org/10.1186/s12967-023-04538-0.
29. Jiang K, Cai J, Jiang Q, Loor JJ, Deng G, Li X, et al. Interferon-tau protects bovine endometrial epithelial cells against inflammatory injury by regulating the PI3K/AKT/beta-catenin/FoxO1 signaling axis. *J Dairy Sci*. 2024;**107**(1):555-72. [PubMed ID: 38220437]. https://doi.org/10.3168/jds.2022-22983.
30. Perez-Moreno P, Riquelme I, Bizama C, Vergara-Gomez L, Tapia JC, Brebi P, et al. LINC00662 Promotes Aggressive Traits by Modulating OCT4 Expression through miR-335-5p in Gallbladder Cancer Cells. *Int J Mol Sci*. 2024;**25**(12). [PubMed ID: 38928444]. [PubMed Central ID: PMC11204134]. https://doi.org/10.3390/ijms25126740.
31. Tsunekuni K, Konno M, Haraguchi N, Koseki J, Asai A, Matsuoka K, et al. CD44/CD133-Positive Colorectal Cancer Stem Cells are Sensitive to Trifluridine Exposure. *Sci Rep*. 2019;**9**(1):14861. [PubMed ID: 31619711]. [PubMed Central ID: PMC6795793]. https://doi.org/10.1038/s41598-019-50968-6.
32. Ma XL, Sun YF, Wang BL, Shen MN, Zhou Y, Chen JW, et al. Sphere-forming culture enriches liver cancer stem cells and reveals Stearoyl-CoA desaturase 1 as a potential therapeutic target. *BMC Cancer*. 2019;**19**(1):760. [PubMed ID: 31370822]. [PubMed Central ID: PMC6676608]. https://doi.org/10.1186/s12885-019-5963-z.
33. Ge Q, Zhou C, Zang C, Li C, Hong H, Wang K, et al. MPZL1 suppresses the cancer stem-like properties of lung cancer through beta-catenin/TCF4 signaling. *Funct Integr Genomics*. 2023;**23**(4):304. [PubMed ID: 37726580]. https://doi.org/10.1007/s10142-023-01232-8.
34. Duan H, Liu Y, Gao Z, Huang W. Recent advances in drug delivery systems for targeting cancer stem cells. *Acta Pharm Sin B*. 2021;**11**(1):55-70. [PubMed ID: 33532180]. [PubMed Central ID: PMC7838023]. https://doi.org/10.1016/j.apsb.2020.09.016.
35. Wang J, Yu H, Dong W, Zhang C, Hu M, Ma W, et al. N6-Methyladenosine-Mediated Up-Regulation of FZD10 Regulates Liver Cancer Stem Cells' Properties and Lenvatinib Resistance Through WNT/beta-Catenin and Hippo Signaling Pathways. *Gastroenterology*. 2023;**164**(6):990-1005. [PubMed ID: 36764493]. https://doi.org/10.1053/j.gastro.2023.01.041.
36. Wang Y, Zhao M, Liu J, Sun Z, Ni J, Liu H. miRNA-125b regulates apoptosis of human non-small cell lung cancer via the PI3K/Akt/GSK3beta signaling pathway. *Oncol Rep*. 2017;**38**(3):1715-23. [PubMed ID: 28713974]. https://doi.org/10.3892/or.2017.5808.
37. Chan YT, Zhang C, Wu J, Lu P, Xu L, Yuan H, et al. Biomarkers for diagnosis and therapeutic options in hepatocellular carcinoma. *Mol Cancer*. 2024;**23**(1):189. [PubMed ID: 39242496]. [PubMed Central ID: PMC11378508]. https://doi.org/10.1186/s12943-024-02101-z.
38. Yuregir Y, Kacaroglu D, Yaylaci S. Regulation of Hepatocellular Carcinoma Epithelial-Mesenchymal Transition Mechanism and Targeted Therapeutic Approaches. *Adv Exp Med Biol*. 2024;**1450**:93-102. [PubMed ID: 37452258]. https://doi.org/10.1007/5584_2023_781.
39. Ahmadpour F, Karimi A, Saadatmandfar MM, Karimi S. Suppressing Effect of Human Wharton's Jelly Mesenchymal Stem Cell Secretomes on Oxidative Stress Induced by Breast Cancer Cell Line SK-BR3. *Jentashapir J Cell Mol Biol*. 2023;**14**(4). https://doi.org/10.5812/jjcmb-141019.
40. Tomecka P, Kunachowicz D, Gorczynska J, Gebuza M, Kuznicki J, Skinderowicz K, et al. Factors Determining Epithelial-Mesenchymal Transition in Cancer Progression. *Int J Mol Sci*. 2024;**25**(16). [PubMed ID: 39201656]. [PubMed Central ID: PMC11354349]. https://doi.org/10.3390/ijms25168972.
41. Debnath P, Huirem RS, Dutta P, Palchaudhuri S. Epithelial-mesenchymal transition and its transcription factors. *Biosci Rep*. 2022;**42**(1). [PubMed ID: 34708244]. [PubMed Central ID: PMC8703024]. https://doi.org/10.1042/BSR20211754.
42. Wu L, Lin L, Yu M, Li H, Dang Y, Liang H, et al. Antitumor Activity of USP7 Inhibitor GNE-6776 in Non-Small Cell Lung Cancer Involves Regulation of Epithelial-Mesenchymal Transition, Cell Cycle, Wnt/beta-Catenin, and PI3K/AKT/mTOR Pathways. *Pharmaceuticals*. 2025;**18**(2). [PubMed ID: 40006058]. [PubMed Central ID: PMC11858873]. https://doi.org/10.3390/ph18020245.
43. Bian S, Ni W, Zhu M, Zhang X, Qiang Y, Zhang J, et al. Flap endonuclease 1 Facilitated Hepatocellular Carcinoma Progression by Enhancing USP7/MDM2-mediated P53 Inactivation. *Int J Biol Sci*. 2022;**18**(3):1022-38. [PubMed ID: 35173534]. [PubMed Central ID: PMC8771828]. https://doi.org/10.7150/ijbs.68179.

44. Wang Z, Li R, Yang G, Wang Y. Cancer stem cell biomarkers and related signalling pathways. *J Drug Target*. 2024;**32**(1):33-44. [PubMed ID: 38095181]. https://doi.org/10.1080/1061186X.2023.2295222.
45. Lim JR, Mouawad J, Gorton OK, Bubb WA, Kwan AH. Cancer stem cell characteristics and their potential as therapeutic targets. *Med Oncol*. 2021;**38**(7):76. [PubMed ID: 34050825]. https://doi.org/10.1007/s12032-021-01524-8.
46. Xia P, Liu DH. Cancer stem cell markers for liver cancer and pancreatic cancer. *Stem Cell Res*. 2022;**60**:102701. [PubMed ID: 35149457]. https://doi.org/10.1016/j.scr.2022.102701.
47. Zhou L, Yu KH, Wong TL, Zhang Z, Chan CH, Loong JH, et al. Lineage tracing and single-cell analysis reveal proliferative Prom1+ tumour-propagating cells and their dynamic cellular transition during liver cancer progression. *Gut*. 2022;**71**(8):1656-68. [PubMed ID: 34588223]. https://doi.org/10.1136/gutjnl-2021-324321.
48. Quiroz Reyes AG, Lozano Sepulveda SA, Martinez-Acuna N, Islas JF, Gonzalez PD, Heredia Torres TG, et al. Cancer Stem Cell and Hepatic Stellate Cells in Hepatocellular Carcinoma. *Technol Cancer Res Treat*. 2023;**22**:15330338231163700. [PubMed ID: 36938618]. [PubMed Central ID: PMC10028642]. https://doi.org/10.1177/15330338231163677.
49. Taracha-Wisniewska A, Kotarba G, Dworkin S, Wilanowski T. Recent Discoveries on the Involvement of Kruppel-Like Factor 4 in the Most Common Cancer Types. *Int J Mol Sci*. 2020;**21**(22). [PubMed ID: 33266506]. [PubMed Central ID: PMC7700188]. https://doi.org/10.3390/ijms21228843.
50. Guo B, Zhao D, Feng J, Liu Y. LncRNA HEIH/miR-4500/IGF2BP1/c-Myc Feedback Loop Accelerates Bladder Cancer Cell Growth and Stemness. *Bladder Cancer*. 2022;**8**(3):255-67. [PubMed ID: 38993687]. [PubMed Central ID: PMC11181846]. https://doi.org/10.3233/BLC-211544.
51. Mortezaee K, Majidpoor J, Kharazinejad E. Epithelial-mesenchymal transition in cancer stemness and heterogeneity: updated. *Med Oncol*. 2022;**39**(12):193. [PubMed ID: 36071302]. https://doi.org/10.1007/s12032-022-01801-0.
52. Lin J, Song T, Li C, Mao W. GSK-3beta in DNA repair, apoptosis, and resistance of chemotherapy, radiotherapy of cancer. *Biochim Biophys Acta Mol Cell Res*. 2020;**1867**(5):118659. [PubMed ID: 31978503]. https://doi.org/10.1016/j.bbamcr.2020.118659.
53. Sabeel Z, Wang J, Dong J, Liu Y, Yu C, Yang Z. The duality of GSK-3beta in urinary bladder cancer: Tumor suppressor and promoter roles through multiple signaling pathways. *Biochim Biophys Acta Rev Cancer*. 2025;**1880**(3):189324. [PubMed ID: 40258445]. https://doi.org/10.1016/j.bbcan.2025.189324.
54. Wang C, Cao F, Cao J, Jiao Z, You Y, Xiong Y, et al. CD58 acts as a tumor promotor in hepatocellular carcinoma via activating the AKT/GSK-3beta/beta-catenin pathway. *J Transl Med*. 2023;**21**(1):539. [PubMed ID: 37573318]. [PubMed Central ID: PMC10422835]. https://doi.org/10.1186/s12967-023-04364-4.
55. Pan S, Liang S, Wang X. ADORA1 promotes nasopharyngeal carcinoma cell progression through regulation of PI3K/AKT/GSK-3beta/beta-catenin signaling. *Life Sci*. 2021;**278**:119581. [PubMed ID: 33961854]. https://doi.org/10.1016/j.lfs.2021.119581.
56. Shi Y, Xu Y, Yao J, Yan C, Su H, Zhang X, et al. MTHFD2 promotes tumorigenesis and metastasis in lung adenocarcinoma by regulating AKT/GSK-3beta/beta-catenin signalling. *J Cell Mol Med*. 2021;**25**(14):7013-27. [PubMed ID: 34121323]. [PubMed Central ID: PMC8278097]. https://doi.org/10.1111/jcmm.16715.
57. Sun J, Zhang S, Wang M, Cheng H, Wang Y, He S, et al. Cinobufacini enhances the therapeutic response of 5-Fluorouracil against gastric cancer by targeting cancer stem cells via AKT/GSK-3beta/beta-catenin signaling axis. *Transl Oncol*. 2024;**47**:102054. [PubMed ID: 38970916]. [PubMed Central ID: PMC11282984]. https://doi.org/10.1016/j.tranon.2024.102054.
58. Basu B, Karmakar S, Basu M, Ghosh MK. USP7 imparts partial EMT state in colorectal cancer by stabilizing the RNA helicase DDX3X and augmenting Wnt/beta-catenin signaling. *Biochim Biophys Acta Mol Cell Res*. 2023;**1870**(4):119446. [PubMed ID: 36791810]. https://doi.org/10.1016/j.bbamcr.2023.119446.
59. Zhu Y, Gu L, Lin X, Cui K, Liu C, Lu B, et al. LINC00265 promotes colorectal tumorigenesis via ZMIZ2 and USP7-mediated stabilization of beta-catenin. *Cell Death Differ*. 2020;**27**(4):1316-27. [PubMed ID: 31527801]. [PubMed Central ID: PMC7206056]. https://doi.org/10.1038/s41418-019-0417-3.